# Type-II WS2-ReSe2 Heterostructure and its Charge Transfer Properties

Xiuxiu Han<sup>1</sup>, Lu Zhang<sup>1</sup>, Dawei He<sup>1</sup>, Shengcai Hao<sup>1</sup>, Shuangyan Liu<sup>1</sup>,

Jialu Fu<sup>1</sup>, Qing Miao<sup>1</sup>, Jiaqi He<sup>2</sup>, Yongsheng Wang<sup>1, \*</sup>, Hui Zhao<sup>3, \*</sup>

<sup>1</sup>Key Laboratory of Luminescence and Optical Information, Ministry of Education,

Institute of Optoelectronic Technology, Beijing Jiaotong University,

Beijing 100044, China; yshwang@bjtu.edu.cn

<sup>2</sup> College of Mathematics and Physics, Beijing University of Chemical Technology,

Beijing 100029, China

<sup>3</sup> Department of Physics and Astronomy, The University of Kansas,

Lawrence, Kansas 66045, United States; huizhao@ku.edu

### Abstract

We fabricated a van der Waals heterostructure of WS<sub>2</sub>-ReSe<sub>2</sub> and studied its charge transfer properties. Monolayers of WS<sub>2</sub> and ReSe<sub>2</sub> were obtained by mechanical exfoliation and chemical vapor deposition, respectively. The heterostructure sample was fabricated by transferring the WS<sub>2</sub> monolayer on top of ReSe<sub>2</sub> by a dry transfer process. Photoluminescence quenching was observed in the heterostructure, indicating efficient interlayer charge transfer. Transient absorption measurements show that holes can efficiently transfer from WS<sub>2</sub> to ReSe<sub>2</sub> on an ultrafast time scale. Meanwhile, electron

transfer from ReSe<sub>2</sub> to WS<sub>2</sub> was also observed. The charge transfer properties show that

monolayers of ReSe<sub>2</sub> and WS<sub>2</sub> form a type-II band alignment, instead of type-I as predicted

by theory. The type-II alignment is further confirmed by the observation of extended

photocarrier lifetimes in the heterostructure. These results provide useful information for

developing van der Waals heterostructure involving ReSe2 for novel electronic and

optoelectronic applications and introduce ReSe<sub>2</sub> to the family of two-dimensional materials

to construct van der Waals heterostructures.

**Keywords:** semiconducting; optical properties

Introduction

Since the discovery of graphene in 2004 [1], many two-dimensional (2D) materials

have been fabricated and studied [2-4]. One of the most extensively studied 2D material

families is the transition metal chalcogenides (TMDs) [5-7]. Unlike the zero-gap graphene,

TMDs have sizeable electronic bandgaps that are strongly dependent on the thickness,

allowing thickness-tunable electronic and optical properties. With enhanced Coulomb

interactions [8], electrons in 2D TMDs are also strongly coupled to light, resulting in novel

optical properties. Hence, TMDs represent enormous potential in applications such as logic

electronic and optoelectronic devices.

As layered materials, TMDs can be easily exfoliated to monolayers. Different TMD

monolayers can also form van der Waals heterostructures by stacking them together

2

vertically. Such heterostructures can possess excellent optoelectronic properties that are different from their individual components. Recent studies have revealed that 2D heterostructures can offer exciting new physics and optoelectronic functionalities that can be utilized in solar cells [9-11], photocatalysis, and field effect transistors [12-17]. Since the TMD family has a large number of materials, they can form numerous heterostructures through different combinations for new material discovery and exploration. Indeed, the research on 2D TMD heterostructures has been rapidly growing in recent years [18].

Previously, only several 2D TMDs have been extensively studied, namely MoS<sub>2</sub>, WS<sub>2</sub>, MoSe<sub>2</sub> and WSe<sub>2</sub>. Consequently, most studies of 2D TMD heterostructures are on combining materials from this list. However, incorporating more TMD members, especially those with different crystalline structures and electronic properties, will significant expand the horizon of this field. Here we report fabrication of WS<sub>2</sub>-ReSe<sub>2</sub> heterostructures and measurements of their charge transfer properties. WS<sub>2</sub> possesses excellent optical properties among the TMDs [19-21]. Meanwhile, ReSe<sub>2</sub> is a newly emerged member of the TMDs family. Its triclinic unit cell has four Re atoms forming a connected parallelogram-shaped cluster, belonging to the bulk space group of P1 [22-23]. Unlike the commonly studied high-symmetry hexagonal TMDs with in-plane isotropic electrical and optical properties, ReSe<sub>2</sub> shows in-plane anisotropic properties due to the lower symmetry of its distorted lattice structure. The anisotropic electrical and optical properties can have potential applications in polarization-sensitive photodetectors [24-25], integrated polarization controllers (such as waveplates) [26-27] and field-effect transistor s[28-29]. Furthermore, unlike most TMDs, a transition from indirect to direct bandgap is absent in ReSe<sub>2</sub>. So far, studies on ReSe<sub>2</sub> have been mostly focused on increasing its crystalline quality [30-32] and understanding its optical [33] and electrical properties [34]. In contrast, there have been few reports on van der Waals heterostructures constructed by this material and the charge transfer properties involving ReSe<sub>2</sub>.

In this paper, a van der Waals heterostructure was fabricated by stacking together monolayers of WS<sub>2</sub> and ReSe<sub>2</sub>. Photoluminescence quenching was observed in the heterostructure in comparison to the individual monolayers, indicating efficient interlayer charge transfer processes. The charge carrier dynamics of the heterostructure was studied by transient absorption measurements. We found that holes excited in WS<sub>2</sub> can transfer to ReSe<sub>2</sub> on an ultrafast time scale. The long lifetime of the photocarriers in the heterostructure proves that electrons and holes are separated in the two layers. This observation shows that the WS<sub>2</sub>-ReSe<sub>2</sub> heterostructure has a type-II band alignment. The conclusion was further confirmed by the observation of electron transfer from ReSe<sub>2</sub> to WS<sub>2</sub>. This work thus proves efficient charge transfer can occur in this heterostructure, and introduces ReSe<sub>2</sub> to the family of 2D materials to construct van der Waals heterostructures.

#### **Results and Discussion**

Figure 1a shows schematically the heterostructure studied in this work. A ReSe<sub>2</sub> monolayer and a WS<sub>2</sub> monolayer are vertically stacked together to form a hetero-bilayer structure by the van der Waals interlayer coupling. In general, materials can form different

types of electronic energy band alignments, depending on the relative positions of their band extremes. Previously, both type-I and type-II band alignments have been observed in TMD heterostructures. The type-I alignment is formed when the conduction band minimum (CBM) and the valance band maximum (VBM) are both located in the same materials. With this alignment, both electrons and holes populated in the material with smaller bandgap. The spatial overlap of the wavefunctions of electrons and holes facilitates their radiative recombination, and thus type-I band alignment is favorable for light-emitting applications [35-36]. In the type-II alignment, the CBM and the VBM are located in different materials. Because the electrons and holes populate different layers, their lifetime can be significantly extended, which is desirable for light detection or photovoltaic devices [37-38].

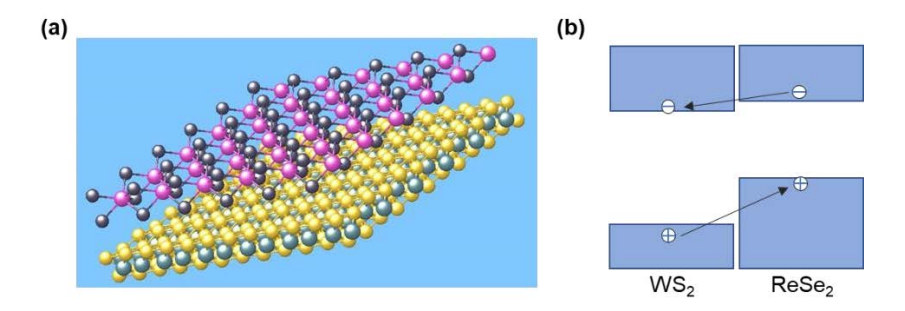
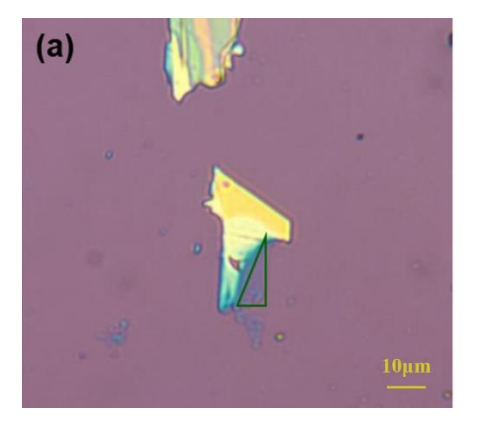


Figure 1: (a) The crystalline structure of the heterostructure sample formed by vertically stacking together monolayers of WS<sub>2</sub> (bottom) and ReSe<sub>2</sub> (top). (b) The band alignment of the WS<sub>2</sub>-ReSe<sub>2</sub> heterostructure and the expected electron and hole transfer processes.

So far, the nature of the band alignment of the WS<sub>2</sub>-ReSe<sub>2</sub> heterostructure is still an open question that requires experimental studies. The central hypothesis and the conclusion of this study is summarized in Figure 1b. We propose that WS<sub>2</sub>-ReSe<sub>2</sub> heterostructure forms

the type-II band alignment, with the CBM and VBM located in the WS<sub>2</sub> and ReSe<sub>2</sub> layers, respectively. Furthermore, due to such an alignment, electrons can efficiently transfer from ReSe<sub>2</sub> to WS<sub>2</sub>, while hole can transfer from WS<sub>2</sub> to ReSe<sub>2</sub>. The transferred electrons and holes are spatially separated in the two layers, resulting in long carrier lifetimes.

According to first-principles calculations, the VBM of ReSe<sub>2</sub> is about 0.3 - 0.4 eV higher than that of WS<sub>2</sub> [36, 39]. Hence, it appears safe to assume that the VBM is located in ReSe<sub>2</sub>. However, the location of the CBM is less certain. Previoous calculations have predicted that the CBM of ReSe<sub>2</sub> is only about 0.04 eV lower than that of WS<sub>2</sub>. [36, 39] This would result in the type-I alignment with both band extremes in ReSe<sub>2</sub>. However, due to the challenges in accurately determining the band structures by the first-principles



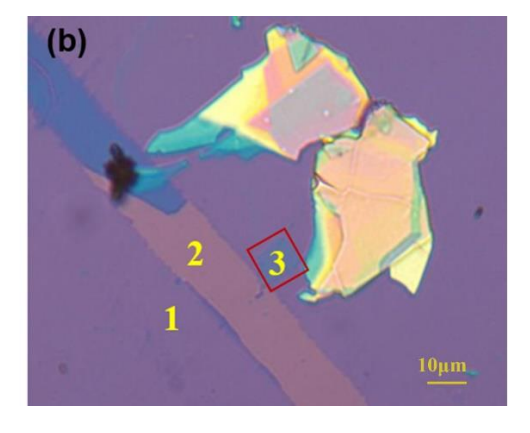


Figure 2: (a) An optical microscope image of the WS<sub>2</sub> flakes. (b) An optical microscope image of the ReSe<sub>2</sub> film and the WS<sub>2</sub>-ReSe<sub>2</sub> heterostructure.

calculations, such a small offset could be within the uncertainties of the theory. Thus, experimental studies on the nature of the band alignment is desirable.

To understand the nature of the band alignment and to probe the charge transfer properties of WS<sub>2</sub>-ReSe<sub>2</sub>, we fabricate samples shown in Figure 2. Figure 2(a) and 2(b) are

the optical microscope images of the monolayer WS<sub>2</sub> and the WS<sub>2</sub>-ReSe<sub>2</sub> heterostructure sample, respectively. The WS<sub>2</sub> monolayer was obtained by mechanical exfoliation from a bulk crystal. The ReSe<sub>2</sub> monolayer film was grown by chemical vapor deposition. The WS<sub>2</sub> monolayer flake was transferred on top of the ReSe<sub>2</sub> film by a dry transfer technique. The samples were thermally annealed to improve the interface quality (see Methods for details). The areas marked 1, 2, 3 in Figure 2(b) are the monolayer ReSe<sub>2</sub>, the Si/SiO<sub>2</sub> substrate, and the WS<sub>2</sub>-ReSe<sub>2</sub> heterostructure, respectively.

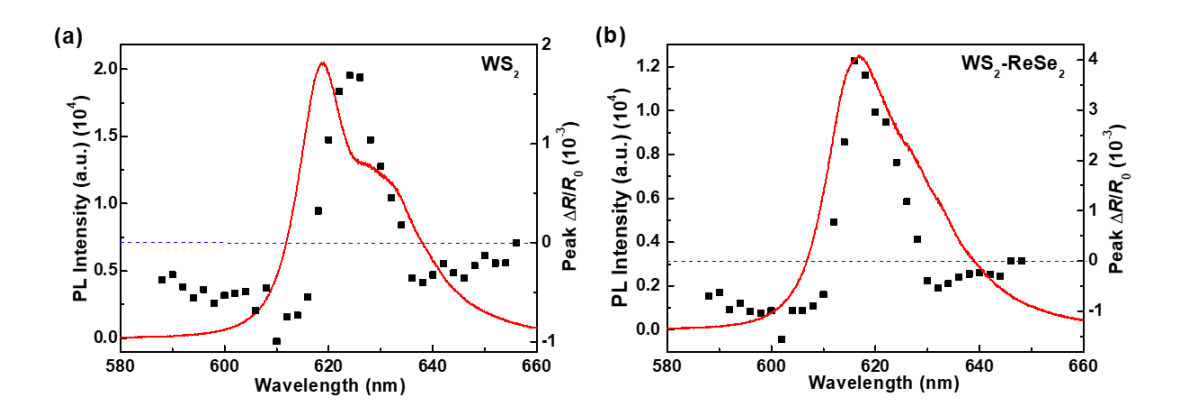


Figure 3: (a) Peak differential reflection signal from the monolayer WS<sub>2</sub> as a function of the probe wavelength (symbols, right axis) and PL of the same sample under 532-nm (2.33-eV) laser excitation. (b) Same as (a) but for the heterostructure sample.

Photoluminescence (PL) spectra of the monolayer WS<sub>2</sub> and the heterostructure at room temperature were obtained under a 532-nm (2.33-eV) laser excitation, as shown as the curves in Figure 3. The peak at about 615 nm and the shoulder at about 625 nm can be attributed to the excitons and trions, respectively. The PL intensity of the heterostructure is

about 60% of the WS<sub>2</sub> monolayer. Since the two spectra were measured under the same conditions, without interlayer interactions, the PL would be similar. The reduction of PL in the heterostructure could thus be attributed to transfer of photocarriers from WS<sub>2</sub> to ReSe<sub>2</sub> before they recombined in WS<sub>2</sub>. Figure 3 also shows the spectra of differential reflection (symbols, right axis). In these measurements, a 410-nm (3.02-eV) pump pulse with a peak fluence of 5.6 µJ cm<sup>-2</sup> was used to inject photocarriers. Differential reflection of the probe with various probe wavelengths was measured as a function of the probe delay. The differential reflection is defined as  $\Delta R/R_0 = (R-R_0)/R_0$ , where R and  $R_0$  are the reflectance of the sample at the probe wavelength with and without the presence of the pump, respectively. The peak differential reflection signal at each probe wavelength is plotted in Figure 3 as the black squares. The strong dependence of the signal near the PL peak proves that in both samples, the differential reflection signal originates from the change of the exciton resonance of WS<sub>2</sub> due to the pump-injected carriers. Therefore, the differential reflection signal monitors population of the photocarriers in WS<sub>2</sub>. The largest signal was obtained with the probes of 1.98 eV and 2.02 eV for the monolayer WS2 and the WS2-ReSe<sub>2</sub> heterostructure samples, respectively. Hence, these probe photon energies will be used in the following experiments.

One way to test our central hypothesis of the type-II band alignment is to observe electron transfer from ReSe<sub>2</sub> to WS<sub>2</sub>, which would prove that the CBM of ReSe<sub>2</sub> is higher than that of WS<sub>2</sub>. We designed an experimental configuration as illustrated in Figure 4(a).

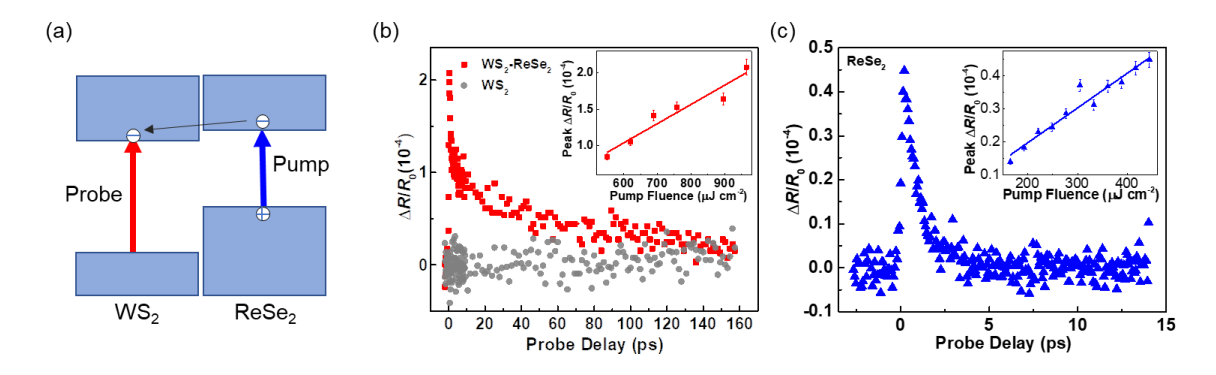


Figure 4: (a) The pump-probe configuration to study electron transfer from ReSe<sub>2</sub> to WS<sub>2</sub>. A 1.51-eV pump excites ReSe<sub>2</sub> only (blue vertical arrow). The excited electrons can transfer to WS<sub>2</sub> if the conduction band minimum of WS<sub>2</sub> is lower than ReSe<sub>2</sub>. The presence of the electrons in WS<sub>2</sub> is detected by a 2.01-eV probe pulse. (b) Differential reflection measured by using the configuration shown in (a) from the WS<sub>2</sub>-ReSe<sub>2</sub> heterostructure (red squares) and the WS<sub>2</sub> monolayer sample (gray circles). The inset shows that the peak signal from the heterostructure is proportional to the pump fluence. (c) Differential reflection signal from a monolayer ReSe<sub>2</sub> measured by using a 2.01-eV pump and a 1.51-eV probe. The inset shows that the peak signal is proportional to the pump fluence.

A less energetic pump of 1.51 eV is used to excite the heterostructure sample. Since its photon energy is far below the optical bandgap of WS<sub>2</sub> of 2.01 eV, it can only excite the ReSe<sub>2</sub> layer, which has a 1.3-eV bandgap. If the electrons excited in ReSe<sub>2</sub> can transfer to WS<sub>2</sub>, they will be sensed by the probe pulse of 2.01 eV. The results of such a measurement are shown in Figure 4(b) as the red squares. The existence of the differential reflection signal in this configuration confirms that electrons excited in ReSe<sub>2</sub> can transfer to WS<sub>2</sub>.

This observation thus proves that the CBM of ReSe<sub>2</sub> is higher than WS<sub>2</sub>, as we hypothesized in Figure 1(b). To confirm our interpretation, three additional measurements were performed to rule out other potential origins of the signal: First, we repeated the measurement on the individual WS<sub>2</sub> monolayer sample, and observed no signal, as indicated by the gray circles in Figure 4(b). This shows that, indeed, the pump does not excite WS<sub>2</sub>. Second, we studied the pump-fluence-dependence of the signal from the heterostructure. As shown in the inset of Figure 4(b), the signal is proportional to the pump fluence. This confirmed that the pump does not excite the WS<sub>2</sub> layer of the heterostructure by two-photon absorption. Indeed, two-photon absorption of WS<sub>2</sub> is negligible at this pump fluence according to previously reported values of its coefficient [40]. Third, to rule out the possibility that the probe senses electrons in the ReSe<sub>2</sub> layer of the heterostructure through mechanisms other than phase-space state filling, such as screening, we studied photocarrier dynamics in an individual ReSe<sub>2</sub> monolayer sample by using the 2.01-eV pulse as the pump and the 1.51-eV pulse as the probe. As shown in Figure 4(c), the dynamics of the photocarriers in ReSe<sub>2</sub> is very different from the signal observed from the heterostructure sample, featuring a very fast decay time. Hence, we conclude that the signal observed from the heterostructure is due to electrons in WS<sub>2</sub>. Since WS<sub>2</sub> is not excited, the only possible origin of these electrons is those transferred from ReSe<sub>2</sub>. Furthermore, the sub-picosecond rising time of the signal indicates that the electron transfer from ReSe<sub>2</sub> to WS<sub>2</sub> occurs on an ultrafast time scale.

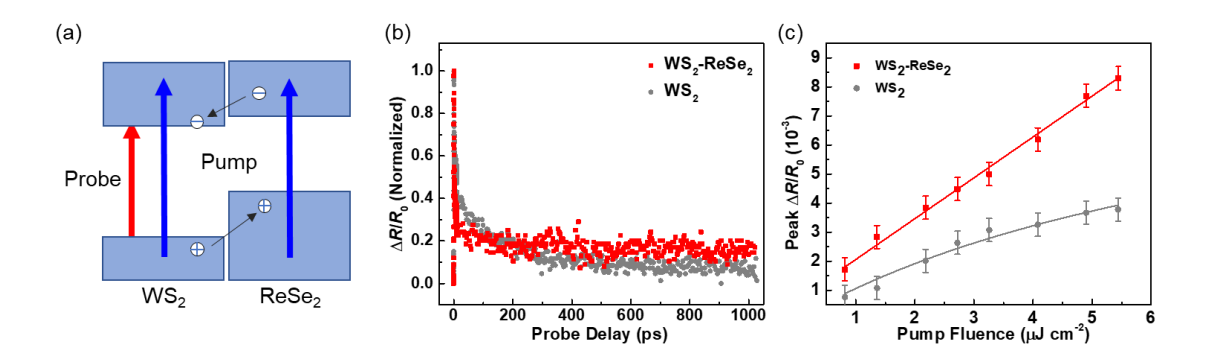


Figure 5: (a) The pump-probe scheme to study hole transfer from WS<sub>2</sub> to ReSe<sub>2</sub> and charge separation. The sample is excited by a 3.02-eV pump pulse and detected by a 2.01-eV probe pulse. (b) Normalized differential reflection signals from the WS<sub>2</sub>-ReSe<sub>2</sub> heterostructure (red squares) and WS<sub>2</sub> monolayer (gray circles). (c) The peak differential reflection signals from the two samples as a function of the pump fluence.

According to theory, the VBM of ReSe<sub>2</sub> is about 0.3 - 0.4 eV higher than that of WS<sub>2</sub> [36, 39]. Thus, the VBM of the heterostructure is located in ReSe<sub>2</sub> and holes excited in WS<sub>2</sub> are expected to transfer to ReSe<sub>2</sub> to lower their potential energy. To study this process, we used the 3.02-eV pump pulse to excite the heterostructure and the 2.01-eV probe to monitor carriers in WS<sub>2</sub>. Figure 5(a) shows schematically the pump -probe scheme and the expected charge transfer. Here, both layers are excited and electrons and holes are expected to transfer along opposite directions and separate into the two layers. The red squares and gray circles in Figure 5(b) show the normalized differential reflection signal from the heterostructure and the WS<sub>2</sub> monolayer, respectively. Clearly, the two samples show different carrier dynamics. The signal from the heterostructure show a slow-decaying

component that persist for more than 1 ns. Such a long carrier lifetime confirms the layer-separation of electrons and holes - a signature of type-II band alignment - and thus hole transfer from WS<sub>2</sub> to ReSe<sub>2</sub>. Furthermore, Figure 5(c) shows the peak signals from the two samples as a function of the pump fluence. For the same fluence, the signal from the heterostructure is about twice of the signal from WS<sub>2</sub>, further confirming the existence of charge transfer. In addition, while the signal from the heterostructure is proportional to the pump fluence (and thus the injected carrier density), a saturation effect was observed in WS<sub>2</sub> [the gray curve in Figure 5(c)]. This can be attributed to different physics mechanisms responsible for the differential reflection signal of the two samples. In the WS<sub>2</sub> monolayer, the signal is caused by excitons and thus mainly through the phase-space state filling effect which has a lower saturation density. In the heterostructure only electrons populate the WS<sub>2</sub> layer and thus their charge screening effect could be significant.

## Conclusion

In summary, we have studied charge transfer in a van der Waals heterostructure fabricated by stacking together monolayers of WS<sub>2</sub> and ReSe<sub>2</sub>. Photoluminescence quenching observed in the heterostructure indicates efficient interlayer charge transfer. The results of transient absorption measurements show that electrons excited in ReSe<sub>2</sub> can transfer to WS<sub>2</sub> on an ultrafast time scale. Meanwhile, holes excited in WS<sub>2</sub> can transfer to ReSe<sub>2</sub>. These observations establish that monolayers of WS<sub>2</sub> and ReSe<sub>2</sub> forms a type-II heterostructure with excellent charge transfer properties. This work introduces ReSe<sub>2</sub> as a

new building block to construct van der Waals heterostructure with good charge transfer properties and provides a strategy for it applications in electronic and optoelectronic devices. Although unexplored in this study, the in-plane anisotropic absorption of ReSe<sub>2</sub> could be utilized in such heterostructures for polarization-sensitive photodetection devices.

#### Methods

The WS<sub>2</sub> bulk crystal used in the experiment was acquired from 2D Semiconductors. A monolayer WS<sub>2</sub> was prepared by mechanical exfoliation from the bulk crystal and then was transferred to a Si/SiO<sub>2</sub> substrate. Another exfoliated monolayer was transferred to a monolayer ReSe<sub>2</sub> film which was grown on a Si/SiO<sub>2</sub> substrate by chemical vapor deposition (acquired from 6 Carbon Technology Corporation, where information about the material characteristics is available). The WS<sub>2</sub>-ReSe<sub>2</sub> heterostructure sample and the monolayer WS<sub>2</sub> sample were both annealed for 6 hours at 200 °C in Ar environment at a base pressure of about 5 Torr.

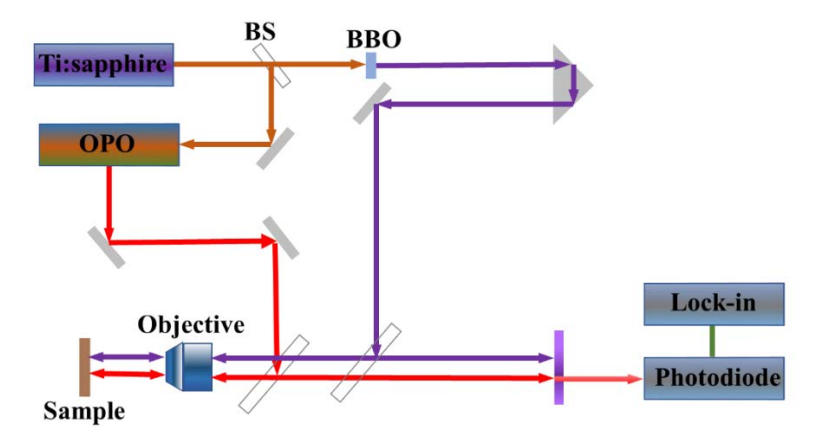


Figure 6: Schematics of the transient absorption setup.

The photocarrier dynamics in these samples was studied by a transient absorption technique [38, 41]. The principle of this technique and the experimental setup have been described previously [42]. Figure 6 shows schematically the experimental configuration. Here, three pulses with wavelengths of 410, 620, and 820 nm were utilized as pump or probe pulses. The 820 nm pulse was obtained from a 80-MHz Ti:sapphire laser. The 410 nm pulse was obtained from second harmonic generation of the 820 nm pulse in a beta barium borate crystal. The 620 nm pulse was obtained from an optical parametric oscillator (OPO) that was pump by the 820 nm pulse. The selected pump and probe beams are combined by a beam splitter (BS) and co-focused to the sample. Their relative arrival time at the sample was controlled by changing the path length of the probe beam with a linear motor stage. In the transient absorption measurements, photocarriers are inject by the pump pulse and monitored by measuring the differential reflection of the probe, which is defined as  $\Delta R/R_0 = (R-R_0)/R$ , where R and  $R_0$  are the probe reflection with the without the pump.

## Acknowledgement

We are grateful for the financial support of National Key RD Program of China (2016YFA0202302), the National Natural Science Foundation of China (61527817, 61875236, 61905010, 61975007), and National Science Foundation of USA (DMR-1505852).

## Reference

- 1. K.S. Novoselov, A.K. Geim., S.V. Morozov, D. Jiang, Y. Zhang, S.V. Dubonos, I.V. Grigorieva, and A.A. Firsov: Electric field effect in atomically thin carbon films. *Science* **306**, 666-669 (2004).
- 2. L. Liao, Y.-C. Lin, M. Bao, R. Cheng, J. Bai, Y. Liu, Y. Qu, K.L. Wang, Y. Huang, and X. Duan: High-speed graphene transistors with a self-aligned nanowire gate. *Nature* 467, 305-308 (2010).
- 3. **K.F. Mak, K.L. McGill, J. Park, and P.L. McEuen**: The valley Hall effect in MoS<sub>2</sub> transistors. *Science* **344**, 1489-1492 (2014).
- 4. J.F. Sherson, H. Krauter, R.K. Olsson, B. Julsgaard, K. Hammerer, I. Cirac, and E.S. Polzik: Quantum teleportation between light and matter. *Nature* 443, 557-560 (2006).
- 5. Q.H. Wang, K. Kalantar-Zadeh, A. Kis, J.N. Coleman, and M. S. Strano: Electronics and optoelectronics of two-dimensional transition metal dichalcogenides. *Nat. Nanotechnol.* 7, 699-712 (2012).
- M. Xu, L. Liang, M. Shi, H. Chen: Graphene-like two-dimensional materials. *Chem. Rev.* 113, 3766-3798 (2013).
- 7. H. Yuan, X. Wang, B. Lian, H. Zhang, X. Fang, B. Shen, G. Xu, Y. Xu, S.-C. Zhang, H.Y. Hwang, and Y. Cui, Generation and electric control of spin-valley-coupled circular photogalvanic current in WSe<sub>2</sub>. *Nat. Nanotechnol.* **9**, 851-857 (2014).
- 8. **A.D. Yoffe**: Low-dimensional systems: Quantum size effects and electronic properties of semiconductor microcrystallites (zero-dimensional systems) and some quasi-two-

dimensional systems. Adv. in Phys. 42, 173-262 (1993).

- 9. M.-L. Tsai, S.-H. Su, J.-K. Chang, D.-S. Tsai, C.-H. Chen, C.-I. Wu, L.-J. Li, L.-J. Chen, and J.-H. He: Monolayer MoS<sub>2</sub> heterojunction solar cells. *ACS Nano* 8, 8317-8322 (2014).
- 10. J.-M. Yun, Y.-J. Noh, C.-H. Lee, S.-I. Na, S. Lee, S. M. Jo, H.-I. Joh, and D.-Y. Kim: Exfoliated and partially oxidized MoS<sub>2</sub> nanosheets by one-pot reaction for efficient and stable organic solar cells. *Small* 10, 2319-2324 (2014).
- 11. E. Gourmelon, O. Lignier, H. Hadouda, G. Couturier, J.C. Bernede, J. Tedd, J. Pouzet, and J. Salardenne: MS<sub>2</sub> (M=W,Mo) photosensitive thin films for solar cells. *Sol. Energ. Mat. Sol. C.* 46, 115-121 (1997).
- 12. Z. Yin, H. Li, H. Li, L. Jiang, Y. Shi, Y. Sun, G. Lu, Q. Zhang, X. Chen. and H. Zhang: Single-layer MoS<sub>2</sub> phototransistors. *ACS Nano* 6, 74-80 (2011).
- 13. S. Cui, H. Pu, S.A. Wells, Z. Wen, S. Mao, J. Chang, M.C. Hersam, and J. Chen: Ultrahigh sensitivity and layer-dependent sensing performance of phosphorene-based gas sensors. *Nat. Commun.* **6**, 8632 (2015).
- 14. **O. Lopez-Sanchez, D. Lembke, M. Kayci, A. Radenovic, and A. Kis**: Ultrasensitive photodetectors based on monolayer MoS<sub>2</sub>. *Nat. Nanotechnol.* **8**, 497-501 (2013).
- 15. **B. Radisavljevic, M.B. Whitewich, and A. Kis**: Integrated circuits and logic operations based on single-layer MoS<sub>2</sub>. *ACS Nano* **5**, 9934-9938 (2011).
- 16. **B.W.H. Baugher, H.O.H. Churchill, Y. Yang, and P. Jarillo-Herrero**: Optoelectronic devices based on electrically tunable p–n diodes in a monolayer dichalcogenide. *Nat.*

Nanotechnol. 9, 262-267 (2014).

- 17. R. Cheng, S. Jiang, Y. Chen, Y. Liu, N. Weiss, H.-C. Cheng, H. Wu, Y. Huang, and X. Duan, Few-layer molybdenum disulfide transistors and circuits for high-speed flexible electronics. *Nat. Commun.* 5, 5143 (2014).
- 18. **A.K. Geim and I.V. Grigorieva**: Van der Waals heterostructures. *Nature* **499**, 419-425 (2013).
- 19. Voiry, D.; Yamaguchi, H.; Li, J., et al., Enhanced catalytic activity in strained chemically exfoliated WS<sub>2</sub> nanosheets for hydrogen evolution. *Nature Mater.* 12, 850-5(2013).
- 20. D. Voiry, H. Yamaguchi, J. Li, R. Silva, D.C.B. Alves, T. Fujita, M. Chen, T. Asefa, V.B. Shenoy, G. Eda, and M. Chhowalla: Vertical field-effect transistor based on graphene-WS<sub>2</sub> heterostructures for flexible and transparent electronics. *Nat. Nanotechnol.* 8, 100-103 (2013).
- 21. Y. Gong, J. Lin, X. Wang, G. Shi, S. Lei, Z. Lin, X. Zou, G. Ye, R. Vajtai, B.I. Yakobson, H. Terrones, M. Terrones, B.K. Tay, J. Lou, S.T. Pantelides, Z. Liu, W. Zhou, and P.M. Ajayan: Vertical and in-plane heterostructures from WS<sub>2</sub>/MoS<sub>2</sub> monolayers. *Nat. Mater.* 13, 1135-1142 (2014).
- 22. H.J. Lamfers, A. Meetsma, G.A. Wiegers, and J.L. de Boer: The crystal structure of some rhenium and technetium dichalcogenides. *J. Alloys Comp.* **241**, 34-39 (1996).
- 23. N.W. Alcock and A. Kjekshus: The crystal structure of ReSe<sub>2</sub>. *Acta. Chem. Scand.* 19, 79-94 (1965).

- 24. S. Yang, S. Tongay, Q. Yue, Y. Li, B. Li, and F. Lu: High-performance few-layer Modoped ReSe<sub>2</sub> nanosheet photodetectors. *Sci. Rep.* **4**, 5442 (2014).
- 25. X. Wang, L. Huang, Y. Peng, N. Huo, K. Wu, C. Xia, Z. Wei, S. Tongay, and J. Li: Enhanced rectification, transport property and photocurrent generation of multilayer ReSe<sub>2</sub>/MoS<sub>2</sub> p–n heterojunctions. *Nano Res.* **9**, 507-516 (2015).
- 26. E. Zhang, P. Wang, Z. Li, H. Wang, C. Song, C. Huang, Z.-G. Chen, L. Yang, K. Zhang, S. Lu, W. Wang, S. Liu, H. Fang, X. Zhou, H. Yan, J. Zou, X. Wan, P. Zhou, W. Hu, and F. Xiu: Tunable ambipolar polarization-sensitive photodetectors based on high-anisotropy ReSe<sub>2</sub> nanosheets. *ACS Nano* 10, 8067-77 (2016).
- 27. S. Yang, S. Tongay, Y. Li, Q. Yue, J.-B. Xia, S.-S. Li, J. Li, and S.-H. Wei: Layer-dependent electrical and optoelectronic responses of ReSe<sub>2</sub> nanosheet transistors.

  Nanoscale 6, 7226-7231 (2014).
- 28. C.M. Corbet, S.S. Sonde, E. Tutuc, and S.K. Banerjee: Improved contact resistance in ReSe<sub>2</sub> thin film field-effect transistors. *Appl. Phys. Lett.* **108**, 162104 (2016).
- 29. **G. Leicht, H. Berger, and F. Levy**, The growth of n-and p-type ReS<sub>2</sub> and ReSe<sub>2</sub> single crystals and their electrical properties. *Solid State Commun.* **61**, 531-534 (1987).
- 30. **Y.S. Huang, C. H. Ho, P.C. Liao, and K.K. Tiong**: Temperature dependent study of the band edge excitons of ReS<sub>2</sub> and ReSe<sub>2</sub>. *J. Alloys Comp.* **262**, 92-96 (1997).
- 31. S. Jiang, M. Hong, W. Wei, L. Zhao, N. Zhang, Z. Zhang, P. Yang, N. Gao, X. Zhou, C. Xie, J. Shi, Y. Huan, L. Tong, J. Zhao, Q. Zhang, Q. Fu, and Y. Zhang: Direct synthesis and in situ characterization of monolayer parallelogrammic rhenium diselenide

on gold foil. Commun. Chem. 1, 17 (2018).

- 32. F. Cui, X. Li, Q. Feng, J. Yin, L. Zhou, D. Liu, K. Liu, X. He, X. Liang, S. Liu, Z. Lei, Z. Liu, H. Peng, J. Zhang, J. Kong, and H. Xu: Epitaxial growth of large-area and highly crystalline anisotropic ReSe<sub>2</sub> atomic layer. *Nano Res.* 10, 2732-2742 (2017).
- 33. C.H. Ho, P.C.Liao, and Y.S. Huang: Optical absorption of ReS<sub>2</sub> and ReSe<sub>2</sub> single crystals. *J. Appl. Phys.* **81**, 6380-6383 (1997).
- 34. **K.K. Tiong, C.H. Ho, and Y.S. Huang**: The electrical transport properties of ReS<sub>2</sub> and ReSe<sub>2</sub> layered crystals. *Solid State Commun.* **111**, 635-640 (1999).
- 35. M.Z. Bellus, M. Li, S.D. Lane, F. Ceballos, Q. Cui, X.-C. Zeng, and H. Zhao: Type-I van der Waals heterostructure formed by MoS<sub>2</sub> and ReS<sub>2</sub> monolayers. *Nanoscale Horiz*. **2**, 31-36 (2017).
- 36. M. Li, M.Z. Bellus, J. Dai, L. Ma, X. Li, H. Zhao, and X.-C. Zeng: A type-I van der Waals heterobilayer of WSe<sub>2</sub>/MoTe<sub>2</sub>. *Nanotechnology* **29**, 335203 (2018).
- 37. X. Hong, J. Kim, S. F. Shi, Y. Zhang, C. Jin, Y. Sun, S. Tongay, J. Wu, Y. Zhang, and F. Wang: Ultrafast charge transfer in atomically thin MoS<sub>2</sub>/WS<sub>2</sub> heterostructures.

  Nature Nanotechnol. 9, 682-686 (2014).
- 38. **F. Ceballos, M.Z. Bellus, H.-Y. Chiu, and H. Zhao**: Ultrafast Charge separation and indirect exciton formation in a MoS<sub>2</sub>-MoSe<sub>2</sub> van der Waals heterostructure. *ACS Nano* **8**, 12717-12724 (2014).
- 39. V.O. Özçelik, J.G. Azadani, C. Yang, S.J. Koester, and T. Low: Band alignment of two-dimensional semiconductors for designing heterostructures with momentum space

matching. Phys. Rev. B 94, 035125 (2016).

- 40. Q. Cui, Y. Li, J. Chang, H. Zhao, and C. Xu: Temporally resolving synchronous degenerate and nondegenerate two-photon absorption in 2D semiconducting monolayers.

  Laser Photonics Rev. 13, 1800225 (2019).
- 41. R. Wang, B.A. Ruzicka, N. Kumar, M.Z. Bellus, H.-Y. Chiu, and H. Zhao: Ultrafast and spatially resolved studies of charge carriers in atomically thin molybdenum disulfide. *Phys. Rev. B* 86, 045406 (2012).
- 42. **F. Ceballos and H Zhao**: Ultrafast laser spectroscopy of two-dimensional materials beyond graphene. *Adv. Funct. Mater.* **27**, 1604509 (2017).